Enhancing the Stability of an Autonomous Microgrid using DSTATCOM

Ritwik Majumder, Arindam Ghosh, Gerard Ledwich and Firuz Zare

ABSTRACT: This paper proposes a method for power sharing in autonomous microgrid with multiple distributed generators (DG). It is assumed that all the DGs are connected through voltage source converter (VSC) and all connected loads are passive, making the microgrid totally inertia less. The VSCs are controlled by either state feedback or current feedback mode to achieve desired voltage-current or power outputs respectively. A modified angle droop is used for DG voltage reference generation. Power sharing ratio of the proposed droop control is established through derivation and verified by simulation results. A distribution static compensator (DSTATCOM) is connected in the microgrid to provide ride through capability during power imbalance in the microgrid, thereby enhancing the system stability. This is established through extensive simulation studies using PSCAD.

I. INTRODUCTION

THE INTERCONNECTION of distributed generators (DGs) through electronic converters to an autonomous microgrid has raised concern of stability due to the lack of inertial generator to provide ride through during transients. This becomes critical if the power generation by some of the DGs suddenly reduces, e.g., when suddenly cloud covers photovoltaic cells. This paper addresses this issue along with proper load sharing during nominal operation. A load sharing with minimal communication is the most desirable in an autonomous microgrid that may span over a large area. The most common method is the use of droop characteristics to deliver desired real and reactive power to the system by the DGs through parallel connected converters. In this case, only local signals are used as feedback to control the converters.

The real and reactive power sharing can be achieved by controlling two independent quantities – the power angle and the fundamental voltage magnitude [1-5]. The system stability during load sharing has been explored in [2, 3]. Transient stability of power system with high penetration level of power electronics interfaced (converter connected) distributed generation is explored in [5].

Application of DSTATCOM in distribution systems has gained considerable attention. While [6] discusses the dynamic performance of a DSTATCOM coupled with an energy storage system (ESS) for improving the power quality of distribution systems, [7] presents a study about the influences of a DSTATCOM on the dynamic behavior of distribution networks. The performance of a DSTATCOM as a voltage controller or a power factor controller is analyzed in [7].

R. Majumder, A. Ghosh, G. Ledwich and F. Zare are with the School of Engineering Systems, Queensland University of Technology, Brisbane, Qld 4001, Australia.

With number of DGs and loads connected to a microgrid spanning over a large area, power balancing through the microgrid is very important for system stability. When the power generation by the DGs is less than the load demand, some of the loads have to be shed. However the load trip command will be executed after a finite time delay that is associated with the circuit breaker open time. Therefore to shed the load properly and to avoid a system collapse, the microgrid voltage needs to be held at its operating value for a few cycles after the load trip command is generated. To provide this voltage support, a DSTATCOM is connected to the microgrid. It is well known that a DSTATCOM can provide reactive power support in normal operation. However, it can release the energy stored in it dc capacitor during transients to provide ride through to facilitate load shedding. In this paper, the effect of sudden power loss is investigated with and without the DSTATCOM connection.

II. MICROGRID STRUCTURE

The structure of the microgrid system studied in this paper is shown in Fig. 1. It contains 9 buses that are separated by feeder segments, 4 DGs, all of which are inertia less and VSC-interfaced, 5 loads and a DSTATCOM. The location of the DSTATCOM is chosen arbitrarily at the center of the microgrid. The feeder impedances are denoted by Z_{ij}, where ij indicates the buses between which these are placed. The DG output voltages are denoted by $E_i\angle\delta_i$, i = 1, …, 4. Each DG and the DSTATCOM are connected to the microgrid through external inductors as shown in Fig. 1. The loads are denoted by Ld_1 to Ld_5. The system data used for the studies are given in Table-I.

TABLE-I: MICROGRID SYSTEM PARAMETERS

System Quantities	Values
Systems frequency	50 Hz
Feeder impedance $Z_{12} = Z_{23} = Z_{34} = Z_{45} = Z_{45} = Z_{56} = Z_{67} = Z_{78} = Z_{89}$	$1.03 + j\,4.71\ \Omega$
Load ratings	
Ld_1	100 kW and 90 kVAr
Ld_2	120 kW and 110 kVAr
Ld_3	80 kW and 68 kVAr
Ld_4	80 kW and 68 kVAr
Ld_5	90 kW and 70 kVAr
DG ratings (nominal)	
DG-1	100 kW
DG-2	200 kW
DG-3	150 kW
DG-4	150 kW
Output inductances	
$L_{G1} = L_{G2} = L_{G3} = L_{G4}$	75 mH
L_S	2 mH

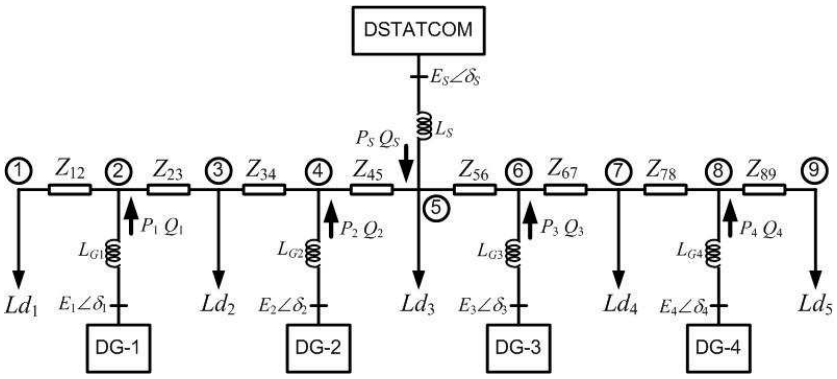

Fig. 1. Structure of the microgrid system under consideration.

III. Converter Structure and Control

The converter structure that is connected to DG-1 is shown in Fig. 2. Here DG-1 is assumed to be an ideal dc voltage source supplying a voltage of V_{dc1} to the VSC. The converter contains three H-bridges. The outputs of the H-bridges are connected to three single-phase transformers that are connected in wye for required isolation and voltage boosting [8]. The resistance R_f represents the switching and transformer losses, while the inductance L_f represents the leakage reactance of the transformers. The filter capacitor C_f is connected to the output of the transformers to bypass switching harmonics, while L_{G1} represents the output inductance of the DG source. The converter structures of all the DG sources and the DSTATCOM are the same. However, the DSTATCOM is supplied by a dc capacitor with an output voltage of V_C.

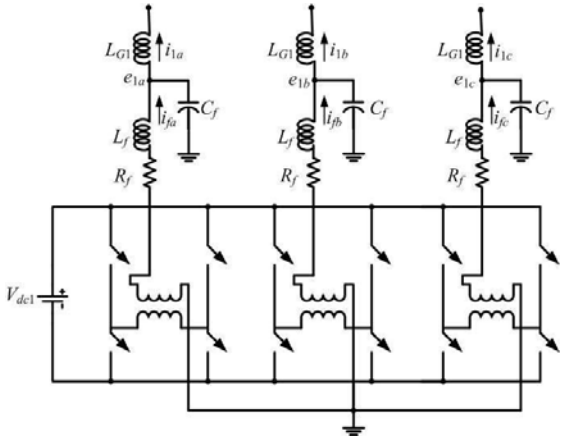

Fig. 2. Converter structure.

The VSC are controlled under closed-loop feedback. Consider the equivalent circuit of one phase of the converter as shown in Fig. 3. In this, $u{\cdot}V_{dc1}$ represents the converter output voltage, where u is the switching function that can take on values ± 1. The main aim of the converter control is to generate u. From the circuit of Fig. 3, the state space description of the system can be given as

$$\dot{x} = Ax + B_1 u_c + B_2 v_{PCC} \tag{1}$$

where u_c is the continuous time control input, based on which the switching function u is determined. The discrete-time equivalent of (1) is

$$x(k+1) = Fx(k) + G_1 u_c(k) + G_2 v_{PCC}(k) \tag{2}$$

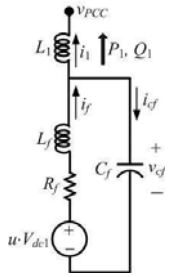

Fig. 3. Equivalent circuit of one phase of the converter.

Neglecting the PCC voltage v_{PCC} assuming it to be a disturbance input, the input-output relationship of the system in (2) can be written in the following two forms

$$\frac{v_{cf}(z)}{u_c(z)} = \frac{M_1(z^{-1})}{N_1(z^{-1})} \tag{3}$$

$$\frac{i_1(z)}{u_c(z)} = \frac{M_2(z^{-1})}{N_2(z^{-1})} \tag{4}$$

The feedback control laws of the converters are generated as discussed below.

A. Control of VSCs Connected to DGs

Under normal operating condition, the VSCs are controlled in state feedback. From Fig. 3, a state vector can be defined as $x^T = [v_{cf}\ \ i_{cf}\ \ i_1]$. The state feedback control law is

$$u_c(k) = K\left[x^*(k) - x(k)\right] \tag{5}$$

where K is the feedback gain matrix and x^* is the reference state vector. In this paper, this gain matrix is designed using LQR method.

When the power output of the DG suddenly reduces or the load demands more than the rated output power from the DG, it is switched to a sinusoidal current limiting mode. In this mode, the output current required to produce the reduced

power or maximum power is set as reference i_1^*. This is then tracked using a pole placement method to compute $u_c(k)$ from (4) [9]. How the references are set for either of the controller will be discussed in the next section.

B. Control of DSTATCOM

The DSTATCOM is controlled in voltage control mode using (3) though pole placement to compute $u_c(k)$ [9]. The magnitude of the reference instantaneous voltage v_{cf}^* is kept fixed, while its angle is determined using the block diagram shown in Fig. 4. First the measured capacitor voltage V_C is passed through a moving average filter with a window of cycle (20 ms) to obtain V_{Cav}. This is then compared with the reference capacitor voltage V_{Cref}. The error is fed to a PI controller to generate the reference angle δ_{Sref}. The instantaneous reference voltages of the three phases are then derived from the pre-specified magnitude and δ_{Sref}.

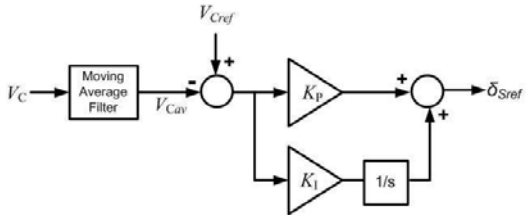

Fig. 4. Angle controller for DSTATCOM.

C. Switching Control

Once $u_c(k)$ is computed from either state feedback or output feedback, the switching function u is generated from

$$\begin{aligned} &\text{If } u_c > h \text{ then } u = +1 \\ &\text{elseif } u_c < -h \text{ then } u = -1 \end{aligned} \tag{6}$$

where h is a small number.

IV. Reference Generation for DG Sources

As mentioned in the previous section, the VSCs connoted to the DGs are either controlled in state feedback or current feedback. The reference generation for these two different control modes is discussed in this section.

A. State Feedback

The output voltages of the converters are controlled to share this load proportional to the rating of the DGs. As the output impedance of the DG sources is inductive, the real and reactive power injection from the source to microgrid can be controlled by changing voltage magnitude and its angle [4].

The power requirement can be distributed among the DGs, similar to conventional droop [4] by dropping the voltage magnitude and angle as

$$\begin{aligned} \delta_1 &= \delta_{1rated} - m_1 \times \left(P_{1rated} - P_1\right) \\ E_1 &= E_{1rated} - n_1 \times \left(Q_{1rated} - Q_1\right) \end{aligned} \tag{7}$$

where E_{1rated} and δ_{1rated} are the rated voltage magnitude and angle respectively of DG-1, when it is supplying the load to its rated power levels of P_{1rated} and Q_{1rated}. The rated angles are determined from the maximum and minimum value of power supplied by the DGs and their load sharing ratio. The coefficients m_1 and n_1 respectively indicate the voltage angle drop vis-à-vis the real power output and the magnitude drop vis-à-vis the reactive power output. These values are chosen to meet the voltage regulation requirement in the microgrid. It is assumed that all the DGs are all converter based and so the output voltage angle can be changed instantaneously. The angle droop will be able to share the load without any drop in system frequency.

From the droop equations given in (7), we can write the angle equation for DG-1 and 2 as,

$$\begin{aligned} \delta_1 &= \delta_{1rated} - m_1 \times \left(P_{1rated} - P_1\right) \\ \delta_2 &= \delta_{2rated} - m_2 \times \left(P_{2rated} - P_2\right) \end{aligned} \tag{8}$$

where P_{2rated} is the real power rating of DG-2. The angle difference then can be written as

$$\begin{aligned} \delta_1 - \delta_2 = \left(\delta_{1rated} - \delta_{2rated}\right) &- m_1 \times \left(P_{1rated} - P_1\right) \\ &+ m_2 \times \left(P_{2rated} - P_2\right) \end{aligned} \tag{9}$$

As the power supply from the DGs to the microgrid is controlled by the source angle, $P_i \propto \delta_i$, $I = 1,2$.

The real power exchange between the DGs is kept constant by maintaining the angle difference constant. Then if we assume $(\delta_1 - \delta_2) = (\delta_{1rated} - \delta_{2rated})$, from (9) we get,

$$m_1 \times \left(P_{1rated} - P_1\right) = m_2 \times \left(P_{2rated} - P_2\right) \tag{10}$$

Now if we choose the droop coefficient such that $m_1 P_{1rated} = m_2 P_{2rated}$, from (10), we get the real power sharing between the two DGs as,

$$m_1 \times P_1 = m_2 \times P_2 \Rightarrow \frac{P_1}{P_2} = \frac{m_2}{m_1} = \frac{P_{1rated}}{P_{2rated}} \tag{11}$$

Similarly, with the voltage magnitude difference are kept constant between the DGs and the droop coefficient for reactive power is taken as $n_1 Q_{1rated} = n_2 Q_{2rated}$, where Q_{2rated} is the reactive power rating of DG-2. In a similar fashion as (8-11), it can be shown that the reactive power sharing between the two DGs is

$$n_1 \times Q_1 = n_2 \times Q_2 \Rightarrow \frac{Q_1}{Q_2} = \frac{n_2}{n_1} = \frac{Q_{1rated}}{Q_{2rated}} \tag{12}$$

Generalizing the observations of (11) and (12), the following power sharing relations between all the four two DGs are obtained

$$\begin{aligned} m_1 \times P_{1rated} &= m_2 \times P_{2rated} = m_3 \times P_{3rated} = m_4 \times P_{4rated} \\ n_1 \times Q_{1rated} &= n_2 \times Q_{2rated} = n_3 \times Q_{3rated} = n_4 \times Q_{4rated} \end{aligned} \tag{13}$$

Once the reference phasor voltage $E_1 \angle \delta_1$ is obtained from the droop equation, the reference phasor current I_{cf} can be obtained (see Fig. 3). Also from the measurement of the bus-2 voltage and P_1 and Q_1, the reference phasor current I_1 can be calculated. The instantaneous quantities can be obtained from these phasor quantities.

B. Current Feedback

As discussed in the previous section when the power output of the DG suddenly reduces or the load demands more than the rated output power from the DG, it is switched to a sinusoidal current limiting mode. Let the maximum available power rating of the DG be denoted by P_{rated} and Q_{rated}. The magnitude and angle of the reference current is calculated from the voltage magnitude ($V_P = V_5$) of the adjacent bus voltage as

$$I_1 = \sqrt{{P_{rated}}^2 + {Q_{rated}}^2} \Big/ V_p$$
$$\beta = \delta_b - \tan^{-1}\left(Q_{rated} / P_{rated}\right) \tag{14}$$

where δ_b is the angle of the adjacent bus (5) voltage. The instantaneous quantities are then generated from these phasor quantities.

V. Simulation Studies

Simulation studies are carried out in PSCAD/EMTDC (version 4.2). Different configurations of load and its sharing are considered. The DGs are considered as inertia-less dc sources supplied through the VSCs. The system data are given in Table-II. The droop coefficients are chosen such that both active and reactive powers of the load are divided in 1:2:1.5:1.5 ratios among DG-1 to DG-4.

TABLE-II: DG, VSC AND CONTROLLER PARAMETERS

System Quantities	Values
DGs and VSCs	
DC voltages (V_{dc1} to V_{dc4})	3.5 kV
Transformer rating	3 kV/11 kV, 0.5 MVA, 2.5% L_f
VSC losses (R_f)	1.5 Ω
Filter capacitance (C_f)	50 μF
Hysteresis constant (h)	10^{-5}
Angle Controller	
Proportional gain (K_p)	– 0.2
Integral gain (K_I)	– 5.0
Droop Coefficients	
Power–angle	
m_1	0.1 rad/MW
m_2	0.05 rad/MW
m_3	0.075 rad/MW
m_4	0.075 rad/MW
Voltage–Q	
n_1	0.04 kV/MVAr
n_2	0.02 Kv/MVAr
n_3	0.03 Kv/MVAr
n_4	0.03 Kv/MVAr

A. Case-1: Load Sharing of the DGs

For the first four cases, the DSTATCOM is not connected to the system. It is further assumed that all the four DGs are able to supply their maximum rated power. As evident from Table-I that the total load demand is less than the total maximum generation. Therefore the DGs will share the load power and the line losses as per the droop coefficients. The results of the real power sharing is shown in Fig. 5 where load 5 (Ld_5) is disconnected at 0.5 s. It can be seen that the power is shared as per the DG ratings. Even though DG-3 and DG-4 ratings are same, there is a slight difference between the power supplied by these DGs due to the line losses and load locations.

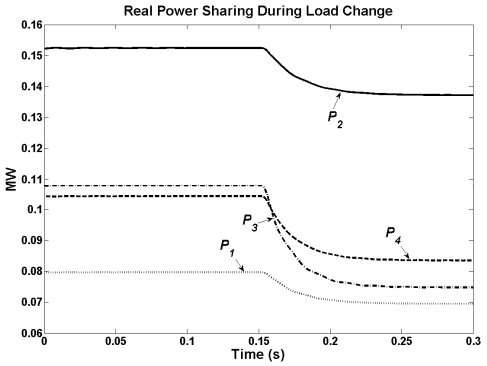

Fig. 5. Real and reactive power sharing for Case-1.

B Case-2: DG output Power Limit

With the DGs operating in steady state sharing the power as in Case-1, the output power from DG-1 suddenly drops to 20 kW at 0.1 s. It can be seen from Table-I that the total load requirement is still less that the total generation even with the reduction of DG-1 power. It is therefore expected that DG-1 will supply 20 kW, while the other three DGs will share the reaming power demand proportional to their rating. This is evident from Fig. 6 (a). Fig. 6 (b) shows the three phase output currents of DG-1, which is operating in current control mode from 0.1 s. It can be seen that despite the switch from state feedback to output feedback control mode, the current settles to the steady state value within half a cycle.

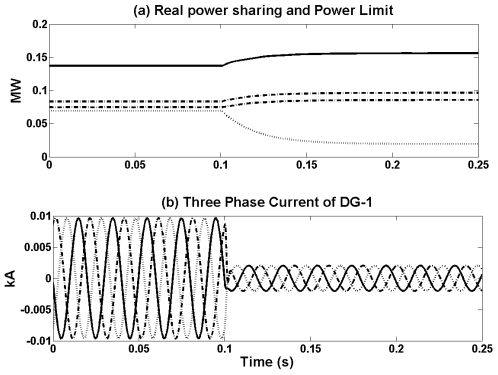

Fig. 6. Real and reactive power sharing for Case-2.

C. Case-3: DG Power Limit and System Instability

Let us investigate what happens when the power generation is less than the power demand. For this we start the system from Case-2, i.e., the output power of DG-1 reduces to 20 kW at 0.1 s. Subsequently at 0.3 s, the power output of DG-3 reduces to 20 kW. The result is shown in Fig. 7. It can be seen that due to the lack of inertia, the whole system collapses as soon as the power output of DG-3 gets limited. In fact the collapse occurs so rapidly that even a quick load shedding cannot save the system. It is to be noted that when such a collapse occurs, all the DGs will be current limited first and disconnected from the system subsequently. Therefore the dramatic result of Fig. 7 can only be shown in simulation.

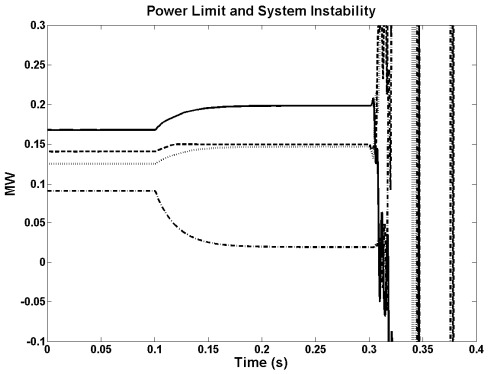

Fig. 7. Real and reactive power sharing (Case-3).

D. Case-4: Load Shedding with DG Output Power Limit

One way of avoiding the total system collapse discussed in Case-3 is to disconnect the load with the least priority once the power output a DG drastically reduces, such as the case when the DG-1 maximum power reduces from 100 kW to 20 kW at 0.1 s. To investigate this, load 2 (Ld_2) is shed from the system at 0.3 s. Subsequently at 0.5 s, the maximum available power from DG-3 is quenched to 20 kW. The result is shown in Fig. 8. It can be seen that the power outputs reduce as load 2 is shed and this provided enough stability margin such that the system remain stable even when the power output of DG-3 reduces.

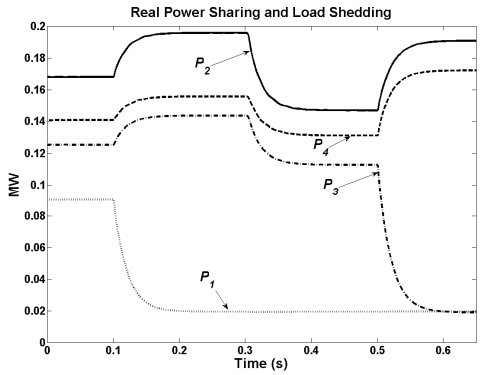

Fig. 8. DG output power limit and load shedding (Case-4).

Even though this preemptive load shedding saves the system from a total collapse, this type of operation might not have much merit when the generation sources are of mixed types. For example, if the generation sources are predominantly PV, then a cloud cover over one may imply that another one will get covered by cloud within a short time. However a cloud cover may not affect microturbines or fuel cells. Thus preemptive load shedding may not always be the correct approach to take. We must therefore provide the microgrid with a storage capability in the form of the DSTATCOM.

E. Case-5: DG Load Sharing with DSTATCOM connected

For the remainder of the cases, it is assumed that the DSTATCOM is connected to the system. Let us first investigate whether the connection has any impact on the load sharing using the droop method. With the system operating in steady state with full load, load 5 is disconnected at 0.5 s. This is the same study as shown in Fig. 5 and the result is shown in Fig. 9. Comparing Fig. 9 with Fig. 5 it can be seen that the discrepancy in the load sharing between DG-3 and DG-4 are the load disconnection in this case is a little bit more than that shown in Fig. 5. However, the load sharing pattern remains the same, indicating that the DSTATCOM has not much impact on the active power sharing.

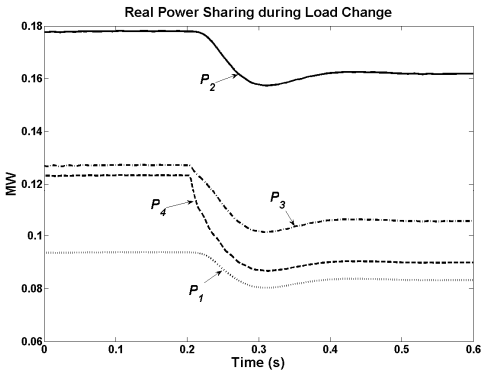

Fig. 9. Real power sharing during load change when the DSTATCOM is connected (Case-5).

F. Case-6: Load Shedding with DSTATCOM

The value of the dc capacitor supplying the DSTATCOM should be so chosen such that there will be no appreciable drop in the dc bus voltage even when the capacitor has to supply power to the microgrid for about four cycles when the power quenching to multiple DGs occurs. After this period, the load shedding occurs and the system is expected to achieve a new steady state. Therefore the energy that is required to be supplied by the dc capacitor (C_{dc}) during the transition period is

$$\frac{1}{2}C_{dc}\left(V_{dc0}^2 - V_{dc1}^2\right) = \int_0^{0.08} P_{load}\, dt \qquad (14)$$

where V_{dc0} is the nominal capacitor voltage, V_{dc1} is the allowable minimum voltage and P_{load} is the average power supplied to the load during the transient. It is assumed that the DSTATCOM has to supply a P_{load} of 200 kW, while the nominal dc voltage is 3.5 kV. If an 85% drop is permissible in the dc voltage (such that V_{dc1} = 3 kV) then from (14) we get C_{dc} = 10000 μF. This value of dc storage capacitor is chosen for the simulation studies.

Fig. 10 shows the system response with DSTATCOM when output power of the DGs reduces and creates a power imbalance in the microgrid. At 0.05 s, DG-1 output power reduces to 20kW and the other DGs share the extra power requirement in a manner similar to that shown in Fig. 7. At 0.35 s, DG-3 power output reduces to 50 kW making the power generation less than the load demand. It can be seen DSTATCOM can hold the system for about 3 cycles. However since no load is shed, the system becomes unstable thereafter. Note that it is possible to hold the microgrid voltage for a longer period of

time by choosing a dc capacitor of bigger size than used here. This however will make the system response very sluggish during any transient.

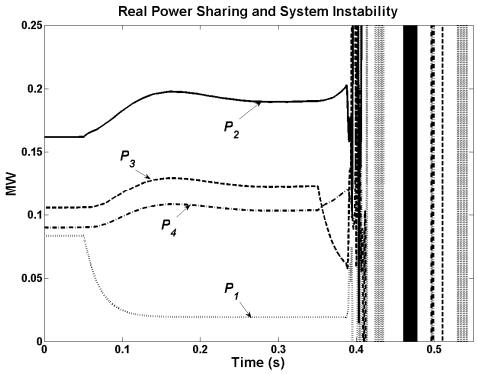

Fig. 10. System instability with DSTATCOM (Case-6)

The above result shows that it is imperative to shed at least a load to make the system stable during power shortfall. To validate this, we shed load-2 (Ld_2) is shed when DG-3 output reduces to 50 kW. As evident from Table-I that even with the reduced generation, the microgrid will be able to supply the other four loads. Fig. 11 shows the system response when load-2 is shed at 0.39s, assuming 2 cycles for the circuit breaker to operate. It can be seen system reaches steady state within 8-9 cycles and DG-2 and DG-4 supply the rest of the power requirement proportional to their rating.

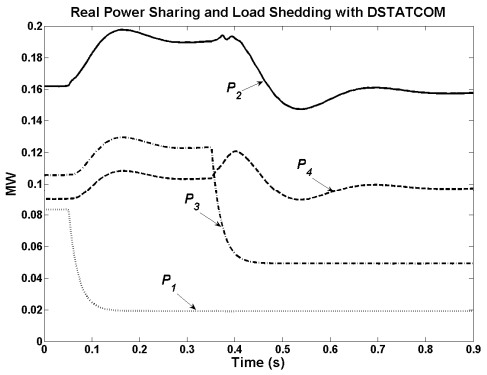

Fig. 11. Load Shedding with DSTATCOM (Case-6).

VI. Conclusions

In this paper, a load sharing technique in an autonomous microgrid with multiple DGs is described. The droop control of voltage angles ensures proper load sharing without any drop in the system frequency. A DSTATCOM is used to enhance the stability of the system. During power imbalance in the microgrid, the DSTATCOM holds the microgrid voltage for few cycles and allows the protection system to shed load and stabilize the system. A large number of case studies are provided to validate the efficacy of the droop control, as well as the operation of the DSTATCOM.

As mentioned in the previous section, that the size of the dc capacitor determines the time for which the DSTATCOM is able to hold the microgrid voltage during power shortfall. The choice of this capacitor is a trade-off between the ride through time and system response. This has to be pre-determined depending on the detection and breaker opening time. Alternatively, it is also possible to supply the dc bus of the DSTATCOM by a battery bank. In that case, it must be ensured that the battery bank does not supply any real power during the normal operating conditions. Furthermore it must be ensured that the DSATCOM, under these conditions, just draws sufficient power in order to supply its losses and keep the battery bank charged.

Finally, a rapid detection of the load shedding requirement is very crucial for the success of this scheme. As can be seen by from Fig. 10 that if the load is not shed within 2-3 cycles, the system voltages will collapse even when the DSTATCOM tries to hold the microgrid voltage. A performance index has to be chosen that is based on local voltage magnitude and angle. Once this index is beyond a threshold, the load shedding has to be initiated. This has not been attempted in this paper.

Acknowledgement

The authors thank the Australian Research Council (ARC) for the financial support for this project through the ARC Discovery Grant DP 0774092.

References

[1] F. Katiraei and M. R. Iravani, "Power management strategies for a microgrid with multiple distributed generation units," IEEE Trans. on Power Systems, Vol. 21, No. 4, pp. 1821-1831, 2006.

[2] M. Reza, D. Sudarmadi, F. A. Viawan, W. L. Kling, and L. Van Der Sluis, "Dynamic Stability of Power Systems with Power Electronic Interfaced DG," Power Systems Conference and Exposition, PSCE'06, pp. 1423-1428, 2006.

[3] J. M. Guerrero, L. G. de Vicuna, J. Matas, M. Castilla, and J. Miret, "A wireless controller to enhance dynamic performance of parallel inverters in distributed generation systems," IEEE Trans. on Power Electronics, Vol. 19, No. 5, pp. 1205-1213, 2004.

[4] M. C. Chandorkar, D. M. Divan and R. Adapa, "Control of parallel connected inverters in standalone ac supply systems," IEEE Trans. On Industry Applications, Vol. 29, No. 1, pp. 136-143, 1993.

[5] J. G. Slootweg and W. L. Kling, "Impacts of distributed generation on power system transient stability," Power Engineering Society Summer Meeting, 2002 IEEE Vol. 2,, pp. 862-867, 2002.

[6] M.G. Molina and P.E. Mercado, "Control Design and Simulation of DSTATCOM with Energy Storage for Power Quality Improvement," Transmission & Distribution Conference and Exposition: Latin America, TDC, IEEE/PES, pp 1-7, 2006

[7] W. Freitas, A. Morelato, X. Wilsun and F. Sato, "Impacts of AC Generators and DSTATCOM devices on the dynamic performance of distribution systems," IEEE Trans. On Power Delivery, Vol. 20, No. 2, pp. 1493-1501, 2005.

[8] A. Ghosh and A. Joshi, "A new approach to load balancing and power factor correction in power distribution system," IEEE Trans. on Power Delivery, Vol. 15, No. 1, pp. 417-422, 2000.

[9] A. Ghosh, A. K. Jindal and A. Joshi, "Inverter control using output feedback for power compensating devices," Proc. IEEE Asia-Pacific Region-10 Conference TENCON, Bangalore, pp. 49-52, October 2003.